

Numerical Analysis on the Propagation of Circular Crack During Cyclic Indentation of Coated Systems

Eduardo A. Pérez Ruiz

Department of Mechanical Engineering, Polytechnic School, University of São Paulo. Av. Prof. Mello Moraes 2231, 05508-900, São Paulo, (SP) Brazil. Tel 3091-5379 ext 212 Fax 3814-2424 ext 217

E-mail: epr@usp.br

Roberto M. Souza

Department of Mechanical Engineering, Polytechnic School, University of São Paulo. Av. Prof. Mello Moraes 2231, 05508-900, São Paulo, (SP) Brazil. Tel 3091-5379 ext 210 Fax 3814-2424 ext 217

E-mail: roberto.souza@poli.usp.br

Abstract. High stresses and complex stress fields are usually developed in thin films when they are submitted to an indentation. Studies on this subject have proved to be important for the understanding of the mechanical behavior of these films.

This work was developed to study the stress fields obtained when successive indentations are conducted on coated systems. The finite element method (FEM), through the software ABAQUS, was used and axisymmetric bidimensional meshes were selected. During the indentations, a spherical indenter was considered and applied normal loads of 50 N on a system composed by a film with elastic behavior and a substrate with elastic-plastic behavior. The analyses have also considered the possibility and the effects of the propagation of circular cracks initially distributed along the film surface. The results allowed an analysis of the propagation of the circular cracks as a function of the number of indentations carried out and the resulting stress fields.

Keywords: Finite Element Method (FEM); Cyclic Indentation; Thin Films.

1. Introduction

The mechanical behavior of thin films deposited onto structural materials plays an important role in the durability of the coated systems. Frequently, the deposition of a hard thin film provides improvements in the tribological behavior of these systems. For example, hard ceramic thin films are used as protective layers in mechanical applications, such as cutting tools. However, such coverings are brittle and have a high tendency to fracture or to fail along the film/substrate interface (Abdul-Baqi et al 2002).

A simple method to evaluate the mechanical properties of a material is the hardness test. This test, using spherical, conical, or pyramidal indenters, also permits an evaluation of the mechanical characteristics of a film (Thomsen, 1998; Ma, 1995 e Souza, 2001). During the indentation, contact stresses are developed, which are an important factor in the tribological behavior of the system. Those contact stresses may be responsible for film fracture, which, during indentation, usually occurs in the morphologies of radial and/or circular cracks (Ma, 1995; Karimi, 2002 e Thomsen, 1998).

The finite element method (FEM) has been extensively used for the study and evaluation of the contact stresses developed during the indentation of systems with thin films (Kral, 1995; Schwarzer, 1995; Gan, 1996; Weppelman, 1996; Huber, 1998; Thomsen, 1998; Bolshakov, 1998; Begley, 1999; Souza, 1999; Souza, 2001a; Souza, 2001b; Souza, 2001c). Traditionally, analyses are restricted to contact stress distribution during one single indentation. More recently (Souza, 1999; Souza 2001a; Souza 2001b), the numerical analyses also considered the presence and propagation of cracks initially distributed along the film surface.

In this work, the propagation of film cracks was also considered, together with an analysis on the effects of repeated indentations on the contact stresses and crack propagation during indentation.

2. Model Description

The ABAQUS software was used to run the element finite method (FEM) simulations, in which the mesh presented in Fig. (1a) was used. A schematic of the most refined portion of the mesh is presented in Fig. (1b). The Indenter shown in the figure was assumed to be rigid and to apply normal loads on the system. The diameter selected was 1.59 mm (1/16 inch), which is the diameter of Rockwell B, F indenters.

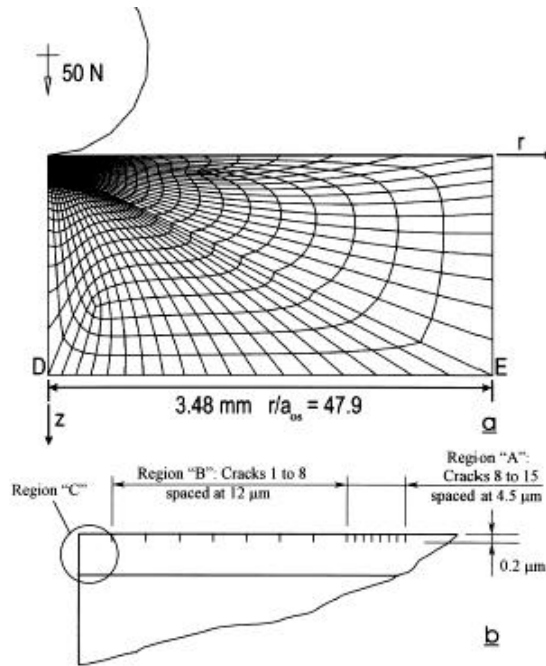


Figure 1. Schematic of mesh used during the element finite analysis. a) Overview; b) Characteristics of the most refined portion of the mesh (Souza, 1999).

13545 four-noded elements were selected to model the coated system. In the model, the substrate had the characteristics of a 6061 aluminum alloy, with elastic-plastic behavior. The elastic and thermal properties for the aluminum (elastic modulus $E = 68.9$ GPa, Poisson ratio $\nu = 0.33$ and coefficient of thermal expansion $\alpha = 23.6 \times 10^{-6} \text{ K}^{-1}$) were taken from a previous work (Souza et al 2001b). The yield strength of the AA 6061 alloy ($\sigma_y = 295$ MPa) was directly obtained from tensile test experiments (Souza et al 2001a). ABAQUS does not require the calculation of the strain-hardening exponent (n) to define the plastic behavior of the substrate.

The film layer of wear resistant material was assumed to be elastic and to present a thickness of $4.6 \mu\text{m}$. The film Poisson ratio was assumed to be 0.3, the elastic modulus was 280 GPa, and the coefficient of thermal expansion was assumed to be equal to $9.8 \times 10^{-6} \text{ K}^{-1}$, which was previously reported as the value of TiN (Souza et al 2001b). The value selected for the film fracture toughness ($K_{IC} = 4.0 \text{ MPa} \sqrt{\text{m}}$) was slightly higher than those used in the previous work (Souza et al 2001b), but remains in the order of magnitude of the fracture toughness of wear resistant thin films.

Different steps were used to load the system. Initially, a uniform biaxial stress was imposed on the films elements to account for the intrinsic stresses that result from the film processing. A compressive value of 0.74 GPa was selected, although it is recognized that larger values were reported for PVD processes. In the second loading step, it was assumed that the temperature reached during deposition was 498 K. Thermal residual stresses were then calculated when the system was cooled to room temperature (298 K). In the third step, a normal load was gradually applied on a reference node on the indenter Fig. (1a). The stresses during indentation were calculated both at maximum load and after the system was unloaded. The third step was repeated to provide a total of five indentation cycles.

In terms of defect size (Fig (1b)), the actual initial crack length value depends on the quality of the film, but for the uniformity of the analyses, an initial crack size $c_0 = 0.2 \mu\text{m}$ was considered reasonable and adopted for the study. During the indentation, the superficial cracks were allowed to propagate in pure mode I along a predetermined path perpendicular to the interface. The ABAQUS criterion for crack propagation was the maximum stress, according to which the cracks in the film were allowed to propagate when a critical stress value was reached at a given position ahead of crack tip. Previous analysis have shown that the consideration of mode II affects the propagation of circular cracks only when crack size has exceeded 1/3 of film thickness (Weppelmann, 1996; Souza, 2001c). Therefore, for the initial crack size, the absence of a mode II criterion does not affect the initial propagation of the 15 circular cracks shown in Fig. (1b).

Once the FEM analyzes were conducted, calculations provided results such as the amount that each of the 15 cracks propagated during the indentations, or the stress distribution along the film surface or along the film/substrate interface.

3. Results and Discussion

Figure 2 presents the amount of propagation of the 15 cohesive cracks for three analyses conducted in this work (one, two and five indentation cycles).

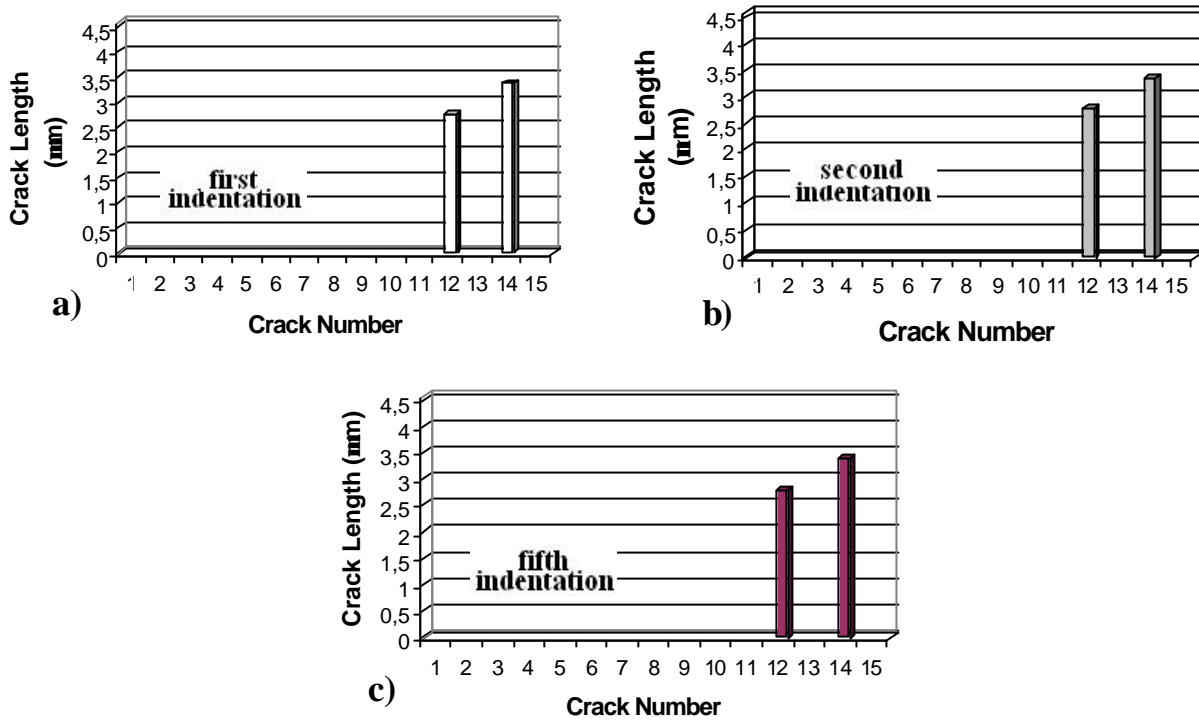


Figure 2. Finite element calculation of the length of each of the 15 cracks distributed over the film surface. Results during cyclic indentations with maximum load of 50 N a) one indentation; b) two indentations; c) five indentations.

The results indicate that for the selected value of film fracture toughness ($K_{IC} = 4.0 \text{ MPa} \sqrt{m}$), the amount of crack propagation was minimal. Only cracks number 12 and 14 propagated after the three conditions of cyclic indentation.

Figure 3 shows the stresses calculated at the maximum load (50 N) of the first normal indentation. Figure (3a) shows the radial (σ_r) stresses along the film surface. Figure (3b) shows the variation of the hoop (S_q) stresses along the film surface. Figure (3c) shows the variation of the radial (σ_r) stresses along the film side of the interface, and Figure (3d) presents the variation of the hoop (S_q) stresses along the film side of the interface.

In all cases the results for the radial distance and stresses were normalized by the values of the radius of contact ($a_{os}=72.7 \mu\text{m}$) and the maximum pressure ($p_{os}=4.51 \text{ GPa}$), obtained when a rigid spherical indenter applies a normal force of 50 N on a bulk elastic aluminum substrate.

Figure 4 shows the stresses presented in Fig. (3), but calculated after the load of the first indentation was entirely released

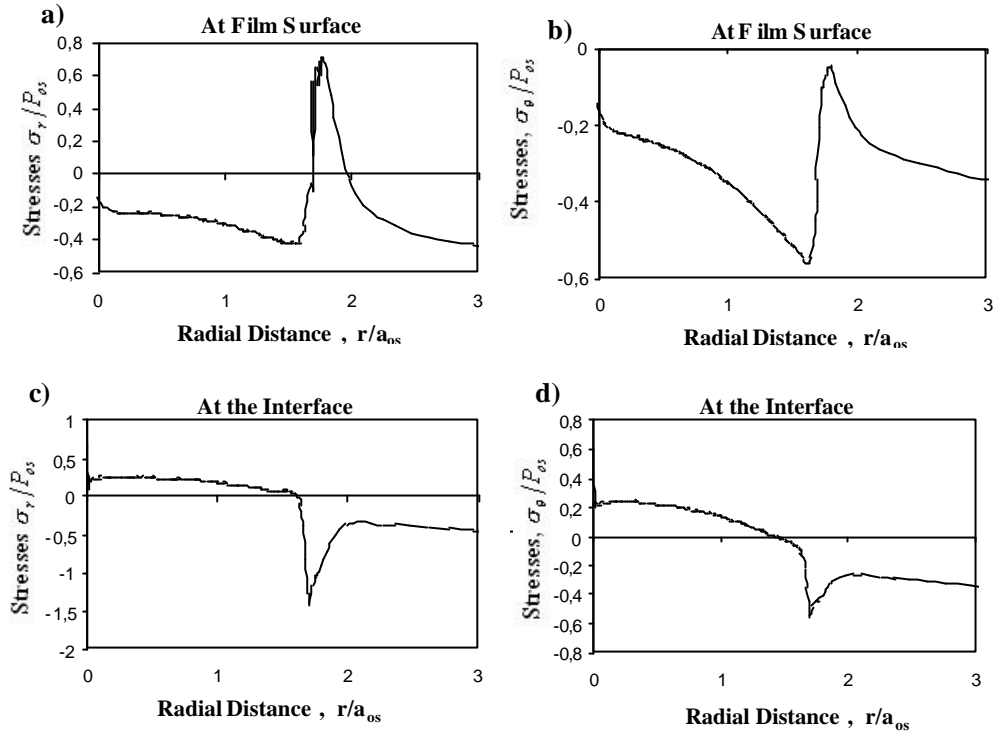


Figure 3. Stresses calculated during the first 50 N normal indentation of system. Values calculated at maximum load. a) radial stresses at the film surface; b) hoop stresses at the film surface; c) radial stresses at the film side of the interface; d) hoop stresses at the film side of the interface.

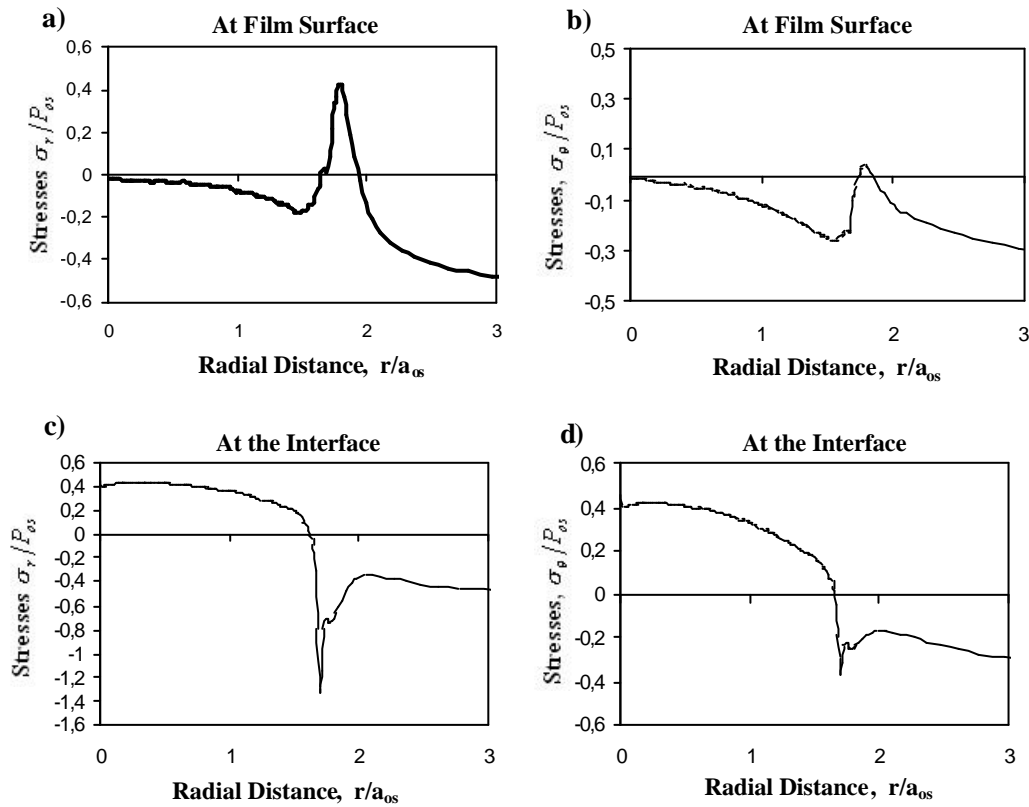


Figure 4. Stresses calculated after the load of the first indentation was entirely released. a) radial stresses at the film surface; b) hoop stresses at the film surface; c) radial stresses at the film side of the interface; d) hoop stresses at the film side of the interface.

The effects of the unloading process (Fig. (4)) have already been discussed by Montmitonnet, 1993 and Souza, 2001a. In those cases, it was verified that unloading results in a movement of S_r and S_q towards more tensile values in regions close to the model axis ($r=0$), which was assumed to be a result of the plastic deformation of the substrate. During unloading, the plastic (permanent) deformation of the substrate should result in additional stresses in the elastic film.

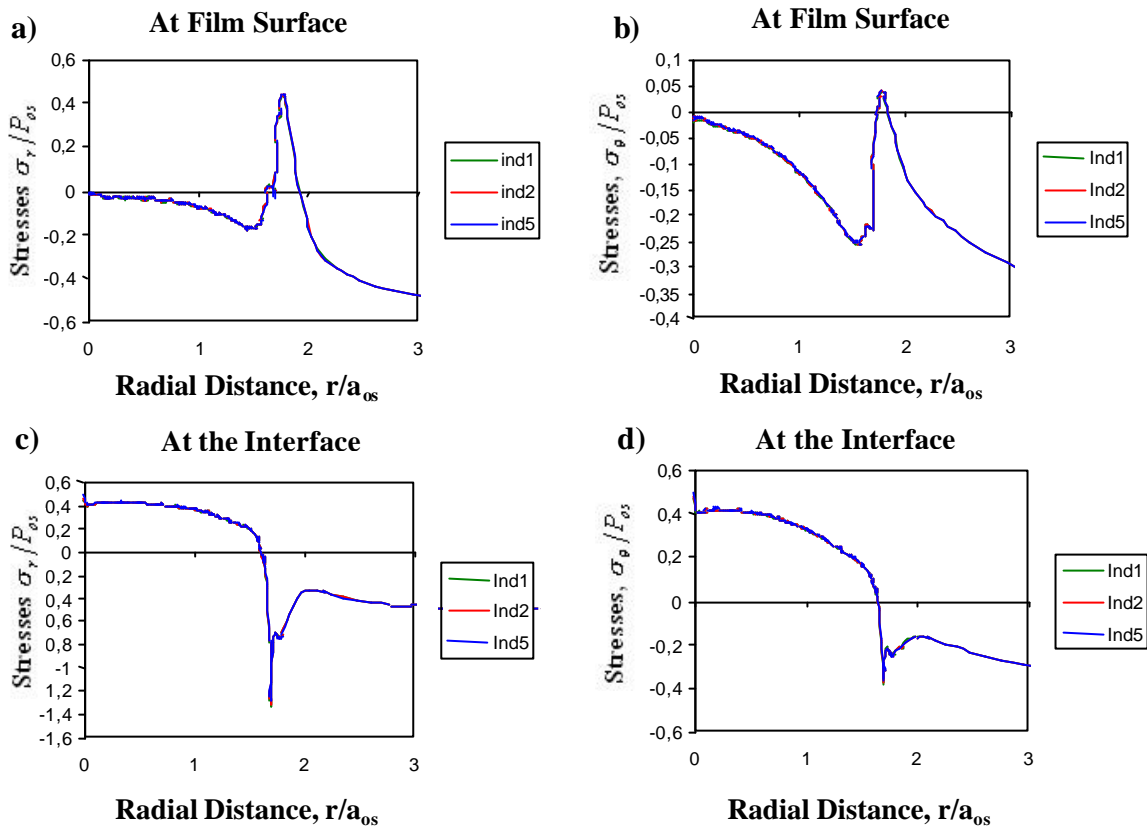


Figure 5. Finite element calculation of the stresses along the film surface. Stresses calculated after the load was entirely released in indentation cycles. a) Radial stresses in the film surface; b) hoop stresses in the film surface, c) Radial stresses in the interface; d) hoop stresses in the interface.

Figure (5) presents the same type of stresses after the unloading conditions of indentations number 1, 2 and 5. Figure (5a) is reproduced in Fig (6), together with a detail of the stresses observed close to the indentation edge ($r/a_{os} \approx 1.8$).

Figures (5) and (6) indicate that only minimal stress variations are observed from the end of one indentation to the end of the next. This fact is in agreement with the absence of differences in amount of crack propagation along the indentations (Fig. (2)).

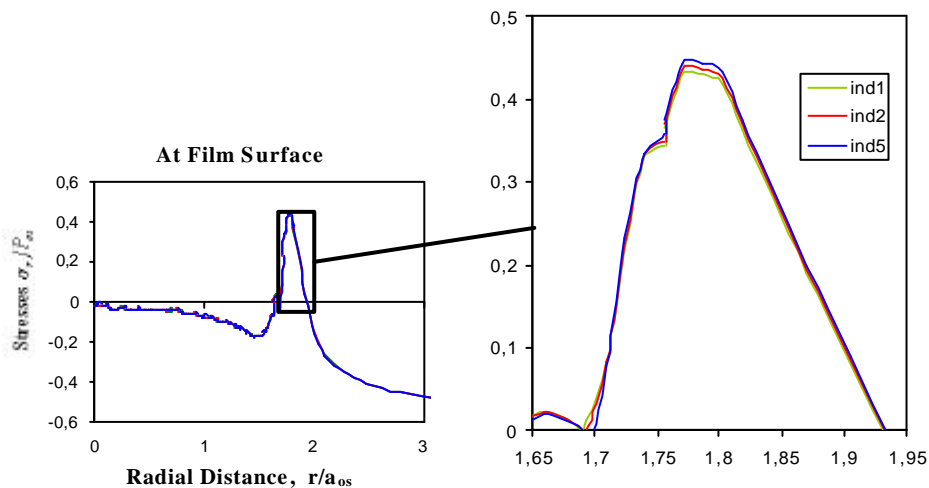


Figure 6. Variation on the distribution of radial stresses in each indentation cycles.

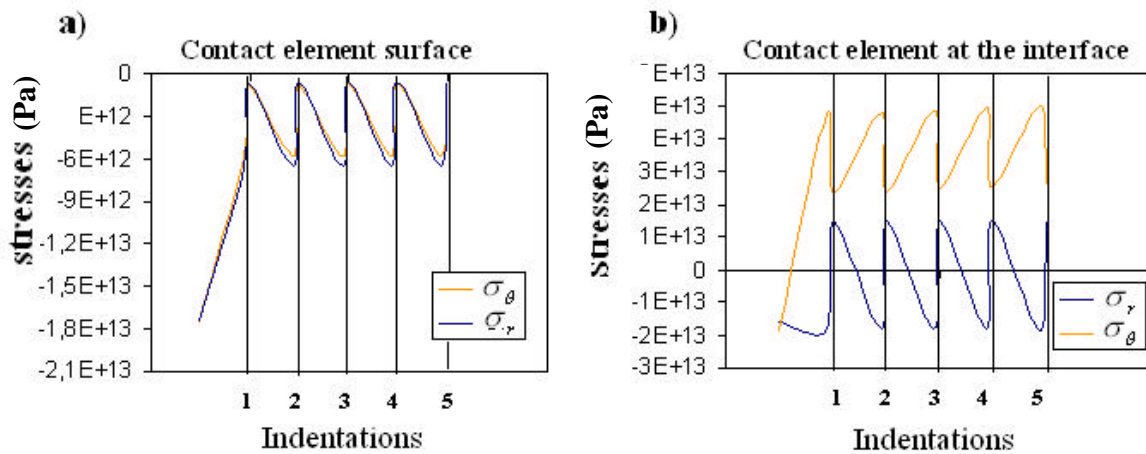


Figure 7. Radial and hoop stresses evolution in the surface and interface of central element contact . a) contact element at surface; b) contact element at the interface.

According to the results in Fig. (6), a slight increase in peak radial stresses at ($r/a_{os} \approx 1.8$) is observed from one indentation to the next. If the same tendency remains in further indentations, a large number of indentation cycles would be required to provide further propagation of the cracks.

Figure (7) presents the evolution of radial and hoop stresses at given positions and along each of the indentations. This figure indicates that, from the beginning of the second indentation, the system behaves almost entirely elastically during loading and unloading steps. Since minimal variations are observed from the end of one indentation to the end of the next one (Fig. (5)), there are limited irreversible phenomena in indentation cycles 2, 3, 4 and 5, which is associated with the plastic deformation of the substrate.

It would be possible to expect that the presence of a longer crack (from indentation number 1) at the beginning of indentation number 2 would result in higher stress intensity factors and further propagation at the second indentation. However, since the analysis is almost entirely elastic during the second indentation (Fig. (7)), the stresses developed at crack tip are similar to those developed in the previous indentation, with similar stress intensity factors at crack tip, therefore no further propagation is observed.

4. Conclusions

In this work, the finite element method was applied to study the effect of cyclic loading on the contact stresses and film crack propagation during indentation. Results have demonstrated that the indentation of coated systems may result in a number of circular cracks inside the contact region of the indentation. The number of cracks propagated after unloading is a function of a peak in radial stresses close to the indentation edge. The results also indicated that, for the conditions studied, significant differences in contact stresses (and amount of crack propagation) were only observed during the first indentation. With the selected conditions, only minimal variations were observed during the subsequent indentations, indicating that a large number of cycles would be necessary to further propagate the film cracks. The changes observed from one indentation to the next were attributed to the plastic deformation of the substrate.

5. Acknowledgements

The author of this work Eduardo A. Pérez R would like to acknowledge to the São Paulo Research Support Foundation (FAPESP) for the financial support through process 01/10864-5.

6. References

- Abdul-Baqi, A., Van der Giessen E., 2002, "Numerical analysis of indentation-induced cracking of brittle coatings on ductile substrate", *International Journal of Solids and Structures*, Vol. 39, pp. 1427-1442
- Begley, M.R., Evans, A.G., Hutchinson, J.W., 1999, "Spherical impression of thin elastic films on elastic-plastic substrates", *International Journal of Solids and Structure*, Vol. 36, pp. 2773-2788
- Bolshakov, A., Pharr, G.M., 1998, "Influences of pileup on the measurement of mechanical properties by load and depth sensing indentation techniques", *Journal of Materials Research*, Vol. 13, pp. 1049-1058
- Gan, L., Ben-Nissan, B., Ben-David, A., 1996, "Modelling and finite element analysis of ultra-microhardness indentation of thin films", *Thin Solid Films*, Vol. 290-291, pp. 362-366
- Huber, N., Tsakmakis, Ch., 1998, "A Finite Element Analysis of the Effect of Hardening Rules on the Indentation Test", *Journal of Engineering Materials and Technology*, Vol. 120, pp. 143-148

- Karimi, A., Wang, Y., Cselle, T., Morstein, M., 2002, "Fracture mechanisms in nanoscale layered hard thin films", *Thin Solid Films*, Vol. 420-421, pp. 275-280
- Kral, E.R., Komvopoulos, K., Bogy, D.B., 1995, "Finite Element Analysis of Repeated Indentation of an Elastic-Plastic Layered Medium by a Rigid Sphere, Part I: Surface Results", *Journal of Applied Mechanics*, Vol. 62, pp. 20-28
- Ma, K.J., Bloyce, A., Bell, T., 1995, "Examination of mechanical properties and failure mechanisms of TiN and Ti-TiN multilayer coatings", *Surface and Coatings Technology*, Vol. 76-77, pp. 297-302
- Montmitonnet, P., Edlinger, M.L. and Felder, E., 1993, "Finite Element Analysis of Elastoplastic Indentation: Part II- Application to Hard Coatings", *Trans. of the ASME - J. of Tribology*, Vol. 115, pp. 15-19
- Schwarzer, N., Djabella, H., Richter, F., Arnell, R.D., 1995, "Comparison between analytical and FEM calculations for the contact problem of spherical indenters on layered materials", *Thin Solid Films*, Vol. 270, pp. 279-282
- Souza, R.M., Mustoe, G.G.W., Moore, J.J., 2001a, "Finite element modeling of the stresses, fracture and delamination during the indentation of hard elastic films on elastic-plastic soft substrates", *Thin Solid Films*, Vol. 392, pp. 65-74
- Souza, R.M., Sinatora, A., Mustoe, G.G.W., Moore, J.J., 2001b, "Numerical and experimental study of the circular cracks observed at the contact edges of the indentations of coated systems with soft substrates", *Wear*, Vol. 251, pp. 1337-1346
- Souza, R.M., Sinatora, A., 2001c, "Study on the effects of mode i and mode ii stress intensity factors on the propagation of cracks located at the surface of coated systems subjected to indentation with normal loads", 16th Brazilian Congress of Mechanical Engineering, Vol. 3, Tribology, pp. 178-186
- Souza, R.M., Mustoe, G.G.W., Moore, J.J., 1999, "Finite element modeling of the stresses and fracture during the indentation of hard elastic films on elastic-plastic aluminum substrates", *Thin Solid Films*, Vol. 355-356, pp. 303-310
- Thomsen, N.B., Fischer-Cripps, A.C., Swain, M.V., 1998, "Crack formation mechanisms during micro and macro indentation of diamond-like carbon coatings on elastic-plastic substrates", *Thin Solid Films*, Vol. 332, pp. 180-184
- Weppelmann, E., Swain, M.V., 1996, "Investigation of the stresses and stress intensity factors responsible for fracture of thin protective films during ultra-micro indentation test with spherical indenters", *Thin Solid Films*, Vol. 286, pp. 111-121

7. Copyright

The authors are the only responsible for the printed material included in this paper.